New Phytologist

Assessing uncertainties in a second-generation dynamic vegetation model caused by ecological scale limitations

Rosie Fisher[1], Nate McDowell[1], Drew Purves[2], Paul Moorcroft[3], Stephen Sitch[4], Peter Cox[5,6], Chris Huntingford[7], Patrick Meir[8] and F. Ian Woodward[9]

[1]Earth and Environmental Science Division, Los Alamos National Laboratory, Los Alamos, NM, USA; [2]Microsoft Research, Cambridge, UK; [3]Department of Organismic and Evolutionary Biology, Harvard University, 22 Divinity Avenue, Cambridge, MA 02138, USA; [4]Department of Geography, University of Leeds, Leeds, UK; [5]School of Engineering, Mathematics and Physical Sciences, University of Exeter, Exeter EX4 4QF, UK; [6]Met Office Hadley Centre, Exeter EX1 3PB, UK; [7]Centre for Ecology and Hydrology, Wallingford, Oxfordshire, OX10 8BB, UK; [8]School of Geosciences, University of Edinburgh, Drummond Street, Edinburgh, UK; [9]Department of Animal & Plant Sciences, University of Sheffield, Sheffield, S10 2TN, UK

Author for correspondence:
Rosie Fisher
Tel: +1 505 6656006
Email: rosieafisher@gmail.com

Received: *16 March 2010*
Accepted: *2 May 2010*

New Phytologist (2010) **187**: 666–681
doi: 10.1111/j.1469-8137.2010.03340.x

Key words: Amazon, competition, competitive exclusion, dynamic global vegetation model (DGVM), ecosystem demography, migration, perfect plasticity, scaling.

Summary

- Second-generation Dynamic Global Vegetation Models (DGVMs) have recently been developed that explicitly represent the ecological dynamics of disturbance, vertical competition for light, and succession. Here, we introduce a modified second-generation DGVM and examine how the representation of demographic processes operating at two-dimensional spatial scales not represented by these models can influence predicted community structure, and responses of ecosystems to climate change.
- The key demographic processes we investigated were seed advection, seed mixing, sapling survival, competitive exclusion and plant mortality. We varied these parameters in the context of a simulated Amazon rainforest ecosystem containing seven plant functional types (PFTs) that varied along a trade-off surface between growth and the risk of starvation induced mortality.
- Varying the five unconstrained parameters generated community structures ranging from monocultures to equal co-dominance of the seven PFTs. When exposed to a climate change scenario, the competing impacts of CO_2 fertilization and increasing plant mortality caused ecosystem biomass to diverge substantially between simulations, with mid-21st century biomass predictions ranging from 1.5 to 27.0 kg C m^{-2}.
- Filtering the results using contemporary observation ranges of biomass, leaf area index (LAI), gross primary productivity (GPP) and net primary productivity (NPP) did not substantially constrain the potential outcomes. We conclude that demographic processes represent a large source of uncertainty in DGVM predictions.

Introduction

The terrestrial biosphere plays a critical role in regulating the Earth's carbon cycle (Bonan, 2008). There is concern that terrestrial ecosystems may be unable to maintain the current uptake of *c.* 33% of anthropogenic emissions (Rodenbeck *et al.*, 2003; Zeng *et al.*, 2005) because of the anticipated negative impact of heating and drying on photosynthesis and survival (Cox *et al.*, 2000; Friedlingstein *et al.*, 2006). For this reason, Dynamic Global Vegetation Models (DGVMs), are now recognized as a critical component of climate change prediction. DGVM models simulate a suite of ecosystem properties from half-hourly carbon and water exchange, through daily growth and tissue turnover, to longer-term processes of reproduction, competition, and mortality. These models have become relatively advanced in their capability to simulate short-term surface gas and energy exchanges and atmospheric CO_2 (Sellers *et al.*, 1986; Hickler *et al.*, 2008; Purves & Pacala, 2008; Mercado *et al.*, 2009; Randerson *et al.*, 2009); by contrast, DGVMs contain relatively simple and poorly tested representations of the processes driving

long-term changes in vegetation composition – for example recruitment, competition and tree mortality (Moorcroft, 2006). The large structural and parametric uncertainty concerning these processes means that existing DGVMs produce a wide variety of predictions regarding the future strength and direction of the climate carbon cycle feedback (Friedlingstein *et al.*, 2006; Thornton *et al.*, 2007; Sitch *et al.*, 2008). For example, some models predict catastrophic declines in the Amazon and Boreal forests, while others predict relatively stable ecosystem composition and carbon storage, even with the same future climate drivers (as illustrated by Sitch *et al.*, 2008). Model biases introduced by these uncertainties are not readily estimated because limited observations exist to constrain demographic processes under rapidly altering climates (Purves & Pacala, 2008; Allen *et al.*, 2010).

In an attempt to increase ecological realism in DGVMs, more sophisticated models have recently been developed that explicitly represent the demographic processes of disturbance, recruitment, competition between plant types for light, and tree mortality (Friend & White, 2000; Moorcroft *et al.*, 2001; Sato *et al.*, 2007; Hickler *et al.*, 2008; Scheiter & Higgins, 2008). This 'second generation' approach has numerous perceived benefits, including the ability to model regrowth after disturbance, parameterize ecological dynamics directly using tree and plot scale data, and to facilitate the representation of coexistence of different vegetation types by introducing different environmental niches, either along a successional gradient of light availability or vertical strata in the canopy (Moorcroft *et al.*, 2001; Smith *et al.*, 2001; Purves & Pacala, 2008). The impact of this third property – the ability to simulate competition and coexistence of multiple plant types – is unclear. Successful coexistence of multiple plant functional types (PFTs) might buffer responses to climate change by preventing sudden switches between mono-dominant PFTs. Conversely, relatively stable past climates might discourage the survival of those plant types which invest more resources in the tolerance of extreme climates, at the expense of PFTs with rapid growth rates, making ecosystems in general more susceptible to the effects of climate shifts.

To resolve this issue, it is necessary to understand the processes that control community structure in second-generation models. In this paper, we present developments to a second-generation DGVM that facilitate the coexistence of plant functional types. We then identify several poorly constrained processes that fundamentally influence how community structure emerges from plant demography. These include seed advection, seed mixing, sapling mortality, competitive exclusion and stress-induced tree mortality. While representations of these ecological processes are typically present in current DGVMs, they all depend upon two-dimensional spatial scales not represented by these models. For example, rates of seed mixing and advection rates are properties of landscape heterogeneity, while the stochasticity or determinism of competitive exclusion and the rate of tree mortality under stress are both properties of multiscale environmental heterogeneity (Clark *et al.*, 2007). DGVMs are spatially one-dimensional, as they consider single points in space that do not interact with one-another. Therefore, it is not possible to explicitly represent these processes in the current modelling context, and instead their impact must be parameterized. In this paper, we identify five demographic processes whose outcome depends on the sub-grid spatial heterogeneity of a landscape, and investigate how the parameterizations affect the outcome of a one-dimensional dynamic vegetation model.

In this paper, we use the Ecosystem Demography model (ED, Moorcroft *et al.*, 2001), a size- and age-structured DGVM that occupies a mid-point on the continuum from gap models (Sato *et al.*, 2007; Hickler *et al.*, 2008) that contain representations of individual trees, to area-based DGVMs, which model the fate of a single average individual for each PFT (Cox, 2001; Bonan *et al.*, 2003; Sitch *et al.*, 2003; Woodward & Lomas, 2004; Krinner *et al.*, 2005). Because of this, ED is perceived as a promising template for a second generation of land surface models, appropriate for inclusion in large-scale climate simulations (Meir *et al.*, 2006; Moorcroft, 2006; Prentice *et al.*, 2007; Huntingford *et al.*, 2008; Purves & Pacala, 2008).

Description

Background

In order to provide a realistic context for our study, we situate our hypothetical ecosystem in the eastern Amazon basin, and parameterize carbon fluxes and plant allocation using recently compiled data from three intensively studied forest plots (Malhi *et al.*, 2009b). Further details are given in Supporting Information Notes S1 and Table 2. A majority of Global Climate Models, (GCMs) predict that dry season rainfall over Amazonia will decline (Malhi *et al.*, 2009a), and that temperatures will increase (Salazar *et al.*, 2007). This makes the Amazon an ideal place to investigate the impact of alternative community structures on future vegetation structure and function. For a more complete review on prognoses for the Amazon rainforest see Cox *et al.* (2004, 2008), Huntingford *et al.* (2008), Malhi *et al.* (2008, 2009b), Meir *et al.* (2008) and Nepstad *et al.* (2008).

Ecosystem Demography model

The ED model is a size- and age-structural approximation of a gap model, the state structure of which is a nested hierarchy of geographical grid cells, landscape age-classes and cohorts of trees of different sizes and PFTs. The landscape age-classes are designed to capture horizontal

biotic heterogeneity in canopy structure that arises from various forms of disturbance. Biotic heterogeneity does not include physical aspects of sub-grid heterogeneity such as variations in altitude, soils or aspect. These are not accounted for in the model structure. At each daily time-step, canopy tree mortality creates new areas of disturbed ground. To make the model computationally more efficient, the spatial locations of the disturbed areas are not specified, and thus can be tracked as a single landscape age-class that represents the aggregation of canopy-gap sized areas within each grid cell that were disturbed at a similar time in the past. To minimize the proliferation of landscape age-classes, the vertical structure and composition of model land classes are continually compared with each other and merged if they are sufficiently similar.

New juvenile individuals of each PFT are recruited on a daily time-step, based on the reproductive output of existing individuals of the same PFT. Individuals located in the same landscape age-class, PFT and size, are tracked as 'cohorts'. Each cohort is defined by the number of individuals per unit area (n_c), and a single representative tree, defined by its structural biomass (b_s), which is a function of tree diameter D (cm), and live biomass (b_a), which consists of leaf (b_l), fine root (b_r) and sapwood (b_{sw}) (all in kg C per individual yr^{-1}). As with the landscape age-classes, cohorts are continually compared and subsequently fused if they are in the same PFT, landscape age-class and are close in size. Through this procedure, the ED model explicitly tracks horizontal and vertical heterogeneity in canopy structure.

In the next section, we discuss model representations of recruitment, competition and mortality. Because these processes operate in two-dimensional spatial space and therefore have no analogue in a one-dimensional model, parameterization from field observations is difficult. We introduced modifications to these processes, but unless otherwise stated, the model is the same as EDv1.0, as described by Moorcroft *et al.* (2001). Alterations made to the energy and gas exchange algorithms are described in Notes S1.

Modelling sapling recruitment

Sapling recruitment is the sum of plant reproduction from local (internal) and nonlocal (external) sources. The smallest units considered by the model are 2.5 m high saplings, we do not model the germination of seeds and early seedling development, but seed dispersal processes are nevertheless responsible for the location of the resultant saplings. External recruitment represents the advection of seeds from other geographical areas. Seed advection (A_s) from multiple directions, results in a point-specific sapling establishment rate measured in individuals m^{-2} per PFT^{-1} yr^{-1}. As the distribution of different environmental conditions within a grid cell is not represented in the model, we use the null assumption that PFT advection is constant through time and that the number of saplings recruited per PFT is equal. For internal recruitment, a fixed fraction, f_{repro} of the carbon available for growth (C_g, Eqn 7) is partitioned into reproduction. The number of saplings per PFT is calculated from this carbon supply divided by the biomass required to make each 2.5 m sapling. The internally generated saplings are distributed between landscape age-classes. This requires an estimate of X_m: the probability that a propagule generated in one landscape age class establishes in a different landscape class from that of its parents. In other words, X_m represents how well mixed seeds are across a landscape with respect to the landscape age-class gradient. Low levels of 'seed mixing' mean that seeds are likely to land near their parent tree, and vice-versa. Subsequently, a 'sapling mortality' is applied (M_s) the value of which represents the discrepancy between the maximum number of saplings and the number that are realized in the model. The total number of new established saplings in each time-step, $N_{sapling}$, is therefore:

$$N_{sapling} = A_s + C_g(1 - M_s)/(f_{repro}\, b_0)\, t \qquad \text{Eqn 1}$$

where t, length of each daily time-step, in years (1/365); and b_0 is the sapling biomass.

The parameters A_s and X_m both depend upon the spatial structure of the landscape and the likelihood of ecosystems with different composition existing in close proximity. In a two-dimensional spatial model of interconnected patches (Kneitel & Chase, 2003; Leibold *et al.*, 2004; Lischke *et al.*, 2006) parameters representing the spatial movement of propagules would not be necessary, as they would be modelled with diffusion type equations; however, without this capacity, we must parameterize the processes of seed dispersal within a grid cell. Here, we investigate how the parameterization of seed advection and seed mixing affect community structure in a sensitivity analysis.

Modelling canopy structure and coexistence

In the original EDv1.0 model (Moorcroft *et al.*, 2001) there were no explicit spatial dimensions associated with each cohort, so the hypothetical leaf area of each tree extended across the entire surface of the landscape age class, effectively creating a steep vertical light profile that caused unrealistic levels of shade-induced competitive exclusion and reduced the capacity to simulate coexistence of plants within a successional age class. Resolving these issues requires representation of the physical dimension of tree crowns. We adopted and modified the Perfect Plasticity Approximation (PPA) of Purves *et al.* (2008b). Based on the observation that tree crowns often occupy gaps in the canopy that are spatially dislocated from the base of the tree,

PPA assumes that the horizontal plasticity of crown location and shape is infinite but that trees have realistic relationships between crown area and height. The end result is that when the total canopy area is greater than the total ground area, the canopy is considered to be 'closed' and breaks into distinct layers, each consisting of those cohorts with heights within a particular range, such that each cohort occurs in only one layer; in a situation with two layers, that is, canopy and understory, the cohorts are assigned to the canopy or understory according to their height relative to a mean canopy intersection height 'z^*'. Trees within the same layer do not shade each other at all and trees in a given layer are uniformly shaded according to the total leaf area index (LAI) above the top height of that layer. This scheme means that a small increase in height of a cohort no longer confers a large competitive advantage, except where cohorts cross z^*.

The original version of the PPA model assumes that z^* is spatially uniform within a stand; however, canopy intersection heights vary spatially such that a tree of height 'h' might sometimes be in the canopy and sometimes be in the understory, depending on its circumstances. The assumption that z^* is spatially uniform, exacerbated by the fact that ED typically aggregates the canopy into far fewer cohorts than the original PPA method of Purves *et al.*, 2008b, generates a highly deterministic model of competition, whereby a single cohort with a small height advantage might come to quickly and unrealistically dominate the entire canopy. It is therefore difficult to represent coexistence between similar PFTs without including some potential for z^* to be heterogeneous. Clark *et al.* (2003, 2007) propose that deterministic models of coexistence often fail because they do not properly account for unobserved life-history trade-offs, neglected genetic variation or spatial heterogeneity in topology, soil type, aspect and dispersal and recruitment processes, they term these factors 'random individual effects'. In the context of the PPA model, this is analogous to the possibility that z^* is spatially heterogeneous.

We introduced the potential influence of 'random individual effects' on community composition by aggregating all the processes that suppress the ability of the fastest growing PFTs to monopolize resources into a single 'competitive exclusion' parameter C_e. This parameter controls the probability that a tree of a given height will obtain a space in the canopy of a closed forest. The forest canopy is considered as closed when the total canopy area (A_{canopy}, m^2), which is the sum of all the crown areas (A_{crown}, m^2)

$$A_{canopy} = \sum A_{crown}, \qquad \text{Eqn 2}$$

exceeds the ground area of the age class in question (A_p). Under these circumstances, the 'extra' crown area A_{loss} ($A_{canopy} - A_p$) is moved into the understorey. For each cohort already in the canopy, we determine a fraction of trees that are lost from the canopy (L_c) and moved to the understory. L_c is calculated as

$$L_c = A_{loss} w_c / \sum (w_c), \qquad \text{Eqn 3}$$

where w_c is a weighting of each cohort determined by basal diameter D (cm) and the competitive exclusion coefficient C_e

$$w_c = D^{C_e} \qquad \text{Eqn 4}$$

The higher the value of C_e, the greater the impact of tree diameter on the probability of a given tree obtaining a position in the canopy layer. That is, for high C_e values, competition is highly deterministic. Small average differences between cohorts are still significant because there is little randomness at the scale of individual trees. Therefore, faster-growing trees monopolize light resources more effectively, leading to competitive exclusion of slower-growing trees. By contrast, low values of C_e imply that the outcome of competition is stochastic: small differences between cohorts do not matter greatly because randomness at the scale of individual trees is such that all cohorts suffer approximately equally from competition for canopy space. The smaller the value of C_e, the greater the influence of random factors on the competitive exclusion process, and the higher the probability that slower-growing trees will get into the canopy. Appropriate values of C_e are poorly constrained (Clark *et al.*, 2003, 2007), thus we investigated the effects of a wide range of C_e values on community structure and biomass predictions.

Modelling plant mortality

Modelling community composition requires accurate simulation of the processes controlling mortality of different plant types. Mechanistic prediction of plant mortality is currently a developing field (McDowell *et al.*, 2008) and the dominant mechanism of death remains unclear. Two potential physiological mechanisms underlying plant susceptibility to climate extremes and attack by biotic mortality agents include hydraulic failure caused by excessive xylem embolism and carbon starvation because of stomatal closure and subsequent depletion of available carbohydrate reserves used for maintenance and defence. Although not yet understood sufficiently well to model, metabolic limitations induced by restrictions on phloem transport and tissue dehydration may exacerbate carbon starvation (Körner, 2003; McDowell & Sevanto, 2010; Sala *et al.*, 2010). Isohydric plants, which close their stomata during drought

conditions, may be more likely to suffer carbon starvation than hydraulic failure (McDowell *et al.*, 2008, Adams *et al.*, 2009). Fisher *et al.* (2006) observed that leaf physiology was consistent with isohydric habit in Amazonian rainforest trees and Metcalfe *et al.* (2010) provide evidence suggesting that the carbon budget and timing of death of artificially droughted rainforest trees is consistent with death from carbon starvation. Therefore, in this paper, we concentrate on carbon starvation as the likely mode of mortality. To simulate carbon starvation, we define a new 'stored carbon' pool, b_{store} (kg C per individual), and model allocation to this pool using the widespread observation that relative partitioning of photosynthate to storage increases during periods when photosynthesis is low (Gibon *et al.*, 2009; McDowell & Sevanto, 2010; Smith & Stitt, 2007). Allocation to the store is thus altered according to the size of the existing pool and a 'target' quantity S^*, multiplied by leaf biomass, b_l. S^* is an indicator of the generic strategy plants undertake to avoid carbon starvation. The more carbon that is kept back for storage, the more likely it is that a plant can survive periods of negative carbon assimilation (McDowell *et al.*, 2008). The carbon balance (C_b) available for storage, growth and reproduction is determined as

$$C_b = \text{NPP} - m_d \qquad \text{Eqn 5}$$

the balance of net primary productivity (NPP) and tissue turnover requirements (m_d, see Notes S1), both in kg C per individual yr^{-1}). The balance of stored carbon to target stored carbon f_s:

$$f_s = b_{\text{store}}/(S^* b_l) \qquad \text{Eqn 6}$$

is used to predict the flux of carbon to the storage pool as a fraction of the carbon balance (f_{store})

$$f_{\text{store}} = e^{-4f_s} \qquad \text{Eqn 7}$$

The form of the function depicts a situation whereby carbon allocation approaches 1.0 when the store is low, and approaches zero when the store is higher than the target quantity. Flux to and from the store is calculated as:

$$\Delta b_{\text{store}} = C_b . f_{\text{store}} \qquad \text{Eqn 8}$$

Thus if C_b is negative (if NPP is less than maintenance demands, such as in winter or drought periods) carbon is removed from the store. Mortality increases as b_{store} declines below a threshold (see Eqn 10), so negative b_{store} is avoided by gradual cohort death. Otherwise, the carbon remaining for growth and reproduction (C_g, kg C per individual yr^{-1}) is what remains once allocation to the store has been removed.

$$C_g = C_b(1.0 - f_{\text{store}}) \qquad \text{Eqn 9}$$

Because each cohort in ED represents the hypothetical means of a set of trees with broadly similar but nonetheless variable genetic composition and environmental conditions, the prediction of mortality based on a single threshold carbon storage value is inappropriate. In this case, we model mortality rate M (fraction of trees dying yr^{-1}) as a function of the ratio of b_{store} to leaf biomass where $b_{\text{store}} < b_l$

$$M = B_m + S_m \min(1.0, (b_l - b_{\text{store}})/b_l) \qquad \text{Eqn 10}$$

Background mortality, B_m, (1.39% yr^{-1}, Chao *et al.* (2008) occurs irrespective of the stress on the carbon store. S_m is the mortality rate (fraction yr^{-1}) of a single cohort when mean cohort carbon storage is zero. The value of S_m is also affected by spatial heterogeneity. In the hypothetical 'average' stand modelled by a DGVM, an 'average' tree may die (making its observed mortality 100%) because its carbon reserves fall to zero. In reality it is unlikely that, across a whole grid cell, all of the trees in a given PFT and size class will die simultaneously. Because we can neither parameterize effectively nor simulate the sub-grid cell heterogeneities that lead to the discrepancy between stand-level and landscape-level mortality, it is necessary to parameterize the variable S_m as the impact of carbon deficit on mortality rates.

Plant functional types

Plant ecology models typically seek to explain the coexistence of species along functional 'trade-offs' (Pacala *et al.*, 1996; Moorcroft *et al.*, 2001; Kneitel & Chase, 2003; Baraloto *et al.*, 2005; Falster 2006). These compromises in plant form and function mean that no species is the best competitor in all environments. We use variation in S^* to represent an example of a growth vs mortality risk trade-off surface (Hacke *et al.*, 2006; Poorter *et al.*, 2010). We constrain S^* using measurements of carbon storage from a rainforest in Panama (Würth *et al.*, 2005), in which the average amount of carbon stored in trees was approximately the same as that required to replace all of the leaf and fine root biomass. Notably, variation between species was substantial. We calculated the range of carbon stored between species using the data on percentage carbon storage in different tissues, and the mean biomass of each tissue type (Würth *et al.*, 2005), and found that carbon storage varied by a factor of 2.4 (or 3.7, if one species with extremely high levels of stem carbohydrate was taken into account). Reflecting this, we created an array of seven tropical, evergreen PFTs that differed in S^* from 1.0 for PFT2, to 2.5 for PFT7 (Table 1). The additional properties of these PFTs are described in Table 2. Each PFT represents a class of species that is broadleaf, evergreen and tropical, but with a specific range of carbon storage behaviour.

Table 1 Value of S^*, the 'target' carbon storage criteria between plant functional types (PPTs)

PFT number	S^*
1	1.0
2	1.25
3	1.5
4	1.75
5	2.0
6	2.25
7	2.5

S^* is the quantity of carbon targeted by the allocation scheme, in multiples of the total leaf biomass (b_l). The range of values chosen is based on observations by Würth *et al.* (2005).

Methods

To develop a DGVM capable of predicting vegetation conditions under altered climate and CO_2, we coupled the adapted ED model to the Met Office Surface Exchange Scheme (MOSES II, Essery *et al.*, 2003), that has recently evolved into joint UK land environment simulator (JULES) (Mercado *et al.*, 2007). JULES calculates the land surface gas exchange and provides fluxes of carbon to ED, which generates land surface and canopy structure to drive the land-atmosphere interactions in return. We term the coupled model JULES-ED.

We drove JULES-ED using output from the IMOGEN analogue climate model (Huntingford & Cox, 2000). IMOGEN utilizes pattern output from the Hadley Centre HADCM3-LC Global Circulation Model (Cox *et al.*, 2000) to provide climatic anomalies between a baseline climate and a given climate change scenario. In this instance, we use the Climate Research Unit (CRU, University of East Anglia, Norwich, UK.) 1900–1999 climatology as a baseline dataset onto which we superimpose these anomalies. In order to use both the historical climatology for spin-up, and the pattern output from the GCM to generate forward predictions, the simulations are not site specific. Instead, we utilize data from Malhi *et al.* (2009b) who synthesized observations of the carbon economy of three Amazonian sites (Manaus, Caxiuanã and Tapajòs) to parameterize the ecophysiology of rainforest ecosystems (see Notes S1). We use driving climatologies for a 3.25 × 2.5 grid cell, the south west corner of which is located at 56.25°W and −2.5°S, encompassing all three sites used by Malhi *et al.* (2009b).

Model sensitivity tests

To investigate how uncertainties in the parameterization of demographic processes affect the development of community structure, we conducted a global sensitivity test to five parameters; seed advection (A_s), seed mixing (X_m), sapling mortality (M_s), competitive exclusion (C_e) and stress-induced adult mortality rate (S_m). For each parameter, we set high and low parameter boundaries and conducted a 200-member Latin Hypercube exploration (Iman & Conover, 1982) of the five-dimensional parameter space to identify how different combinations of these processes affect community structure. The parameter ranges for X_m, C_e and S_m were between zero and one because these were the logical endpoints of these processes. For A_s the minimum input was 0 and the maximum upper limit was 50 individual ha^{-1} yr^{-1}. For M_s the maximum rate was 1.0, while we set the minimum as 95%. The model results described later illustrate that the output appears to be insensitive beyond these ranges for A_s and M_s.

For each ensemble member, we ran the model for 400 yr, starting from bare ground in 1700. For the baseline climatology we use 100 yr of CRU data randomized over these 400 yr (except for the 20th century, where we use actual year numbers). To this we added climate anomalies generated by the IMOGEN model driven CO_2 concentrations from the HADCM3-LC coupled climate carbon

Table 2 Model parameters obtained from literature sources

Parameter	Explanation	Units	Value	Source
M_b	Background mortality	%	1.39	Chao *et al.* (2008)
D	Wood density	g C cm^{-3}	0.7	Chao *et al.* (2008)
a_{leaf}	Leaf turnover	yr^{-1}	0.69	Wright *et al.* (2004)
a_{root}	Fine root allocation	yr^{-1}	0.69	Malhi *et al.* (2009b)
a_{wood}	Coarse wood turnover (branches & coarse roots)	yr^{-1}	0.01	Malhi *et al.* (2009b)
SLA_c	Specific leaf area (canopy)	cm^2 g^{-1}	87	Carswell *et al.* (2002)
SLA_u	Specific leaf area (understory)	cm^2 g^{-1}	145	Carswell *et al.* (2002)
r_r	Root respiration as a fraction of leaf respiration	Fraction	0.50	Malhi *et al.* (2009b)
r_s	Stem respiration as a fraction of leaf respiration	Fraction	0.63	Malhi *et al.* (2009b)
K_N	Exponent of change in nitrogen through canopy	–	0.17	Mercado *et al.* (2007)
N_0	Nitrogen concentration at canopy top	KgN KgC^{-1}	0.046	Mercado *et al.* (2007)
f_{repro}	Fraction of growth carbon to respiration	Fraction	0.37	P Meir *et al.* (unpublished)

cycle model output (Cox *et al.*, 2000; Friedlingstein *et al.*, 2006; Sitch *et al.*, 2008). This climate change scenario is among the most extreme for Amazonia (Malhi *et al.*, 2009a), but appears consistent with recent climate variability in this region (Cox *et al.*, 2004, 2008; Jupp *et al.*, 2010). The annual CO_2, precipitation and temperature components of the model drivers are shown in Fig. 1.

Results and Discussion

Impact of parameter variation on ecosystem biomass responses to climate change

Altering the five demographic parameters that control unconstrained spatially mediated demographic processes had a profound influence on the predicted response of ecosystem biomass to future CO_2 and climate (Fig. 2a). Biomass estimates in 2005 ranged from 6.6 to 22.1 kg C m^{-2} yr^{-1}. By 2050, the competing effects of increasing mortality and productivity in the future scenarios create an even wider divergence in biomass (3.25–27.0 kg C m^{-2} yr^{-1}). Some ensemble members are able to benefit from CO_2 fertilization, while others are more rapidly affected by the increasingly severe drought events (Fig. 1). Between 2059 and 2060, there is a large drought event that depletes the carbon store and causes mortality in even the most conservative plant functional types. By 2100, plant biomass is heavily depleted in most scenarios, with the most resilient scenario supporting 9.6 kg C m^{-2}. The response of LAI to changing climate and CO_2 is both less extreme and differs less between runs as LAI recovers more quickly after disturbance and is therefore less affected by variations in ecosystem demography. We emphasize that, owing to the random selection of baseline climate, this illustration is not meant to be proscriptive of the actual future climate or vegetation in particular years.

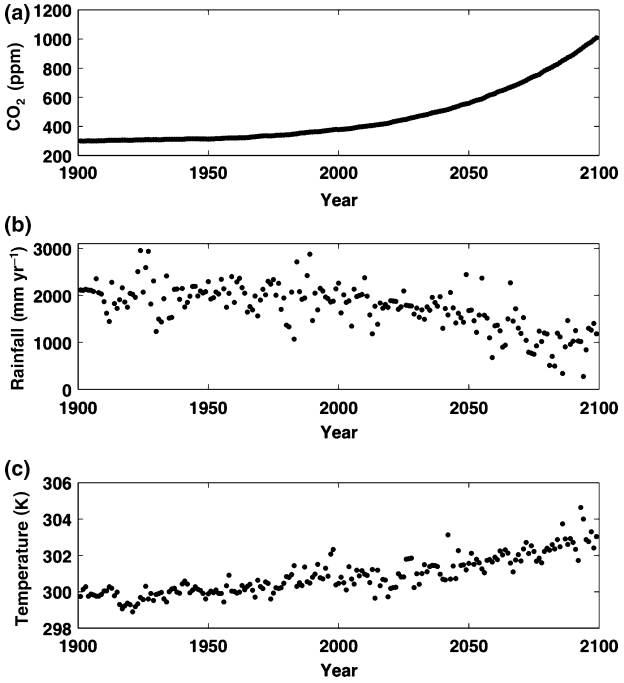

Fig. 1 Forcing data for model simulations: (a) carbon dioxide concentrations, (b) temperature and (c) annual precipitation.

Filtering unrealistic ensemble members

The parameter space exploration generated wide variation in ecosystem properties for the present day (Fig. 2a); however, many of the ensemble members generated unrealistic predictions for ecosystem properties that can be constrained by current observations. We filtered those ensemble members whose biomass, GPP, NPP or LAI fell outside observed ranges (Malhi *et al.*, 2009b; Fisher *et al.*, 2007; Brando *et al.*, 2008). To account for measurement error in the upper and lower boundaries of the observations, we extended the ranges by 10% on either side. After the filtering process, 14 ensemble members remained whose estimates of all four variables were inside the observed ranges (Fig. 2b). While there are many fewer simulations in the filtered set, the spread of predictions is not substantially reduced, with biomass in year 2050 still ranging from 2.6 to 27.0 kg C m^{-2} yr^{-1}. Filtering with this particular set of model metrics did not allow us to constrain the different model futures or rule out either the extremely sensitive or extremely resistant scenarios. Therefore, satisfactory approximation of contemporary ecosystem observations is not necessarily an indicator that a model will produce accurate future predictions. Current efforts to 'benchmark' vegetation models with sets of basic ecosystem data, with the intention of constraining the range of future predictions, should consider this possibility when interpreting their results (Randerson *et al.*, 2009). It is possible that additional filters not used in this experiment, notably responses of forest to experimental drying (Fisher *et al.*, 2007; Brando *et al.*, 2008) might provide more appropriate filtering data. These kinds of plot-level observations are not yet considered in DGVM benchmarking exercises, however, owing to the difficulties involved in precisely replicating the experimental conditions in DGVM models.

Community structure and its relation to ecosystem biomass predictions

Fig. 3 illustrates the different plant community structures found in the 14 runs that met the filtering criteria. The panels are ordered according to their predicted ecosystem biomass in 2050 (from low to high). Those runs where forest mortality events were predicted to occur sooner, and biomass in 2050 was consequentially lower (e.g. Fig. 3 – top

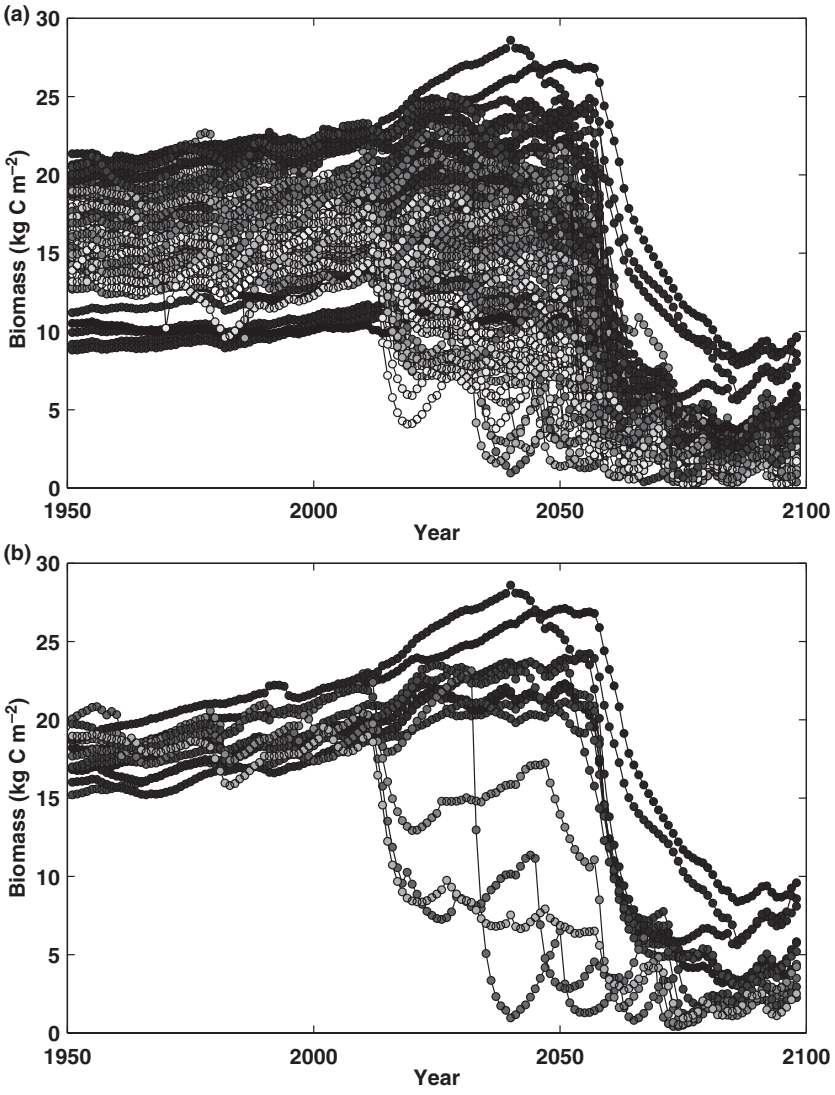

Fig. 2 Response of the trajectory of total plant biomass to alterations in ecological parameterizations showing the last 150 yr of the 400 yr simulation. (a) Includes all 200 members of the ensemble and (b) includes only those 14 ensemble members with acceptable biomass, leaf area index (LAI), gross primary production (GPP) and net primary productivity (NPP) compared with observations. Shading on symbols indicates the sapling mortality (M_s) parameter for each run, and can be read from Fig. 5(d).

two rows), were dominated by the fast-growing PFT 1 (filled circles), while those runs where the ecosystem avoided biomass collapse for longer tended to have a more equitable distribution of PFTs (e.g. Fig. 3 – bottom two rows). In this particular model scenario, prevailing conditions before 2000 typically favour the dominance of the fastest-growing plant types. The persistence of PFT1 as the dominant plant type in 2000 reflects the relatively benign climatic conditions over the last century and is consistent with a small fitness cost associated with low rates of carbon storage: NPP rarely falls sufficiently to deplete stored carbon reserves enough cause canopy tree mortality. In all cases, the fastest-growing PFTs gain a slight initial advantage via lower allocation to carbon storage. The eventual community structure, however, depends upon the strength of processes that reinforce this initial dominance, which is affected substantially by varying the spatially mediated parameters in this sensitivity test.

Impact of individual parameters on community structure and ecosystem properties

Illustrating detailed ecosystem composition for every ensemble member was impractical, so we reduced the dimensionality of the output by calculating a PFT range. R_p, for each model run, as

$$R_p = B_{f,1} - B_{f,7} \qquad \text{Eqn 11}$$

where $B_{f,i}$ is the fractional biomass of the ith PFT in 2000. Fractional biomass is the total of the total biomass accounted for by a given PFT. Values close to 1 indicate dominance the fastest-growing PFT and values close to zero indicate more equitable PFT distribution. This metric of community structure provides a single value with which to represent how much the community is dominated by fast-growing plants. Fig. 4 illustrates how this measure of

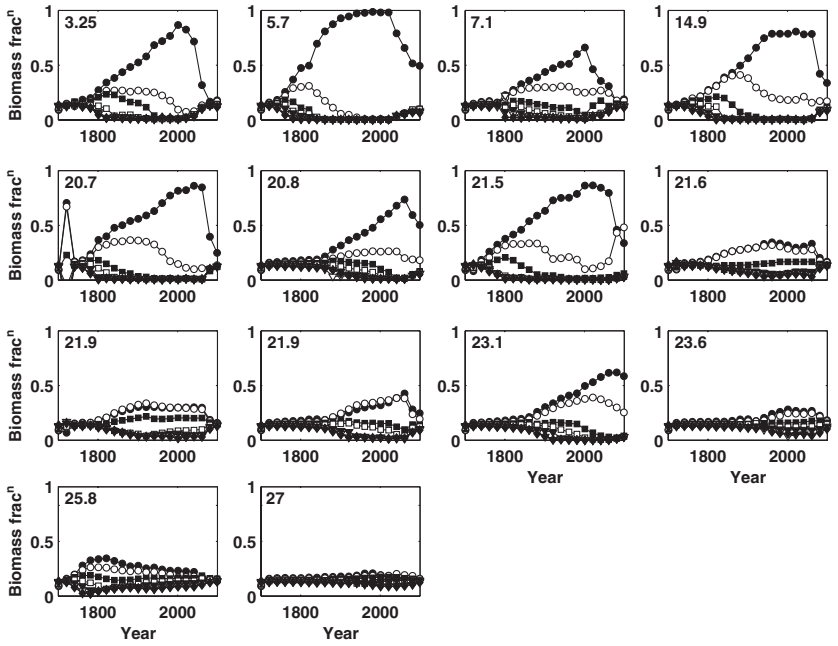

Fig. 3 Development of plant functional type (PFT) community composition over 400 yr model evaluation for each of 16 ensemble members with acceptable values of biomass, gross primary production (GPP), net primary productivity (NPP) and leaf area index (LAI). Panels are arranged according to the biomass predicted in 2050, to illustrate the impact of community composition on ecosystem prediction. Biomass in 2050 for each run is shown in text on each figure. Symbols refer to different PFTs: closed circles, PFT1; open circles, PFT2; closed squares, PFT3; open squares, PFT4; closed triangles, PFT5; open triangles, PFT6; closed diamonds, PFT7; open diamonds, PFT8.

community structure affects whole-ecosystem properties (GPP, NPP LAI and biomass) used in the filtering process. Typically, those ecosystems with a PFT range close to 1 had high values of GPP, NPP and LAI, which were often outside the observational range. Ecosystem biomass was greatest for mid-range community composition. Those ensemble members with highly equitable PFT distribution tended to have very low biomass, below the acceptable range.

Figs 5–7 illustrate how the five demographic parameters that we investigated were related to PFT range index (Eqn 10, Fig. 5), biomass predictions at 2050 (Fig. 6) and LAI in 2005 (Fig. 7). The impact of the different parameters on NPP, GPP and biomass in 2005 and biomass in 2100 are illustrated in Figs S1–S4.

Of the five parameters varied, sapling mortality (M_s) had the greatest impact on community structure and ecosystem properties. To illustrate the impact of varying this parameter on the model output, we shaded the points in Figs 4–7 according to their value of M_s. M_s mediates the positive feedback between fast growth and sapling production. Those trees with fast growth rates produce large numbers of saplings that grow quickly during situations of

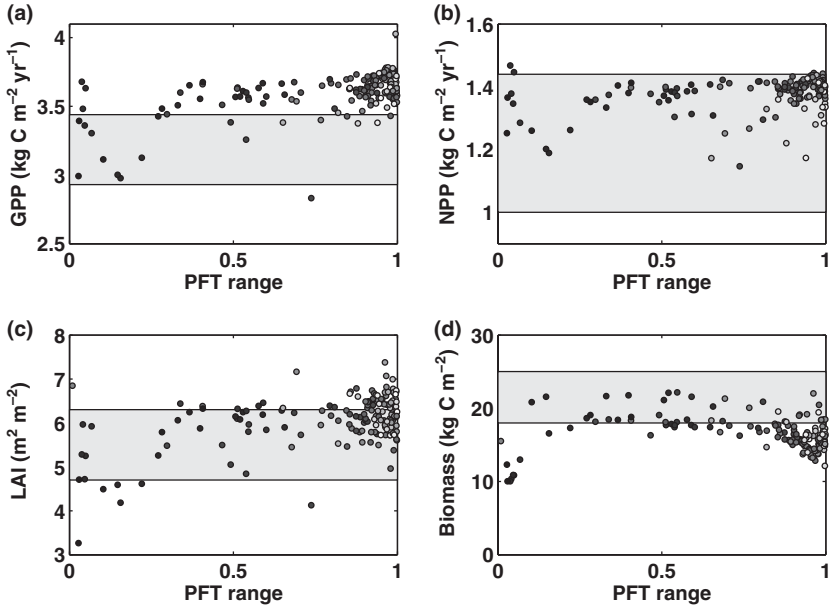

Fig. 4 Relationship between (a) gross primary production (GPP), (b) net primary productivity (NPP), (c) leaf area index (LAI) and (d) biomass in 2005, and ecosystem composition as expressed by the plant functional type (PFT) range metric (Eqn 10). The shaded area indicates the limits of observations. Shading on symbols indicates the sapling mortality (M_s) parameter for each run, and can be read from Fig. 5(d).

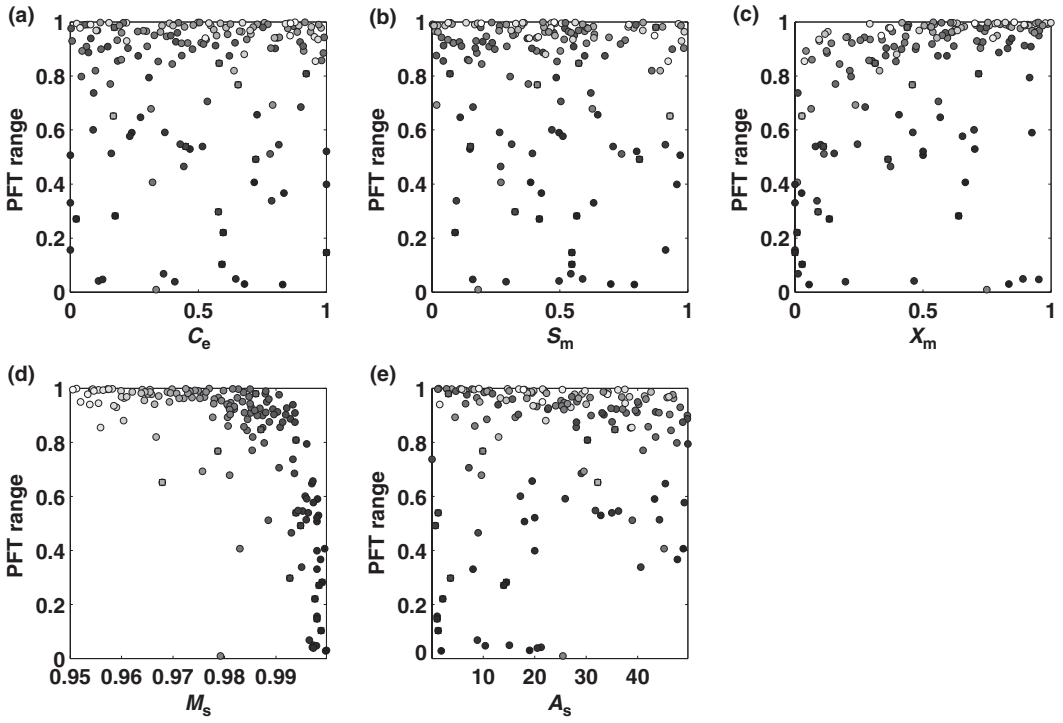

Fig. 5 Response of modelled plant functional type (PFT) range in 2005 to variation in (a) competitive exclusion, C_e, (b) stress-induced adult mortality, S_m, (c) seed mixing, X_m, (d) sapling mortality, M_s, and (e) seed advection, A_s. Shaded area denotes limits of observations from Malhi *et al.* (2009b). Square symbols denote members of the filtered ensemble with predictions of net primary productivity (NPP), gross primary production (GPP), leaf area index (LAI) and biomass within acceptable ranges. Shading on symbols indicates the sapling mortality parameter for each run, and can be read from panel (d).

low sapling mortality, increasing the tendency of fast-growing PFTs to become dominant. Low values of M_s encourage this positive feedback, leading to monodominance and high PFT range. Simulations with high values of M_s suppress this feedback and tended to have a more equitable PFT distribution with more slow-growing PFTs (Fig. 5d). These PFTs are less susceptible to drought induced mortality (in the model), so the runs with high M_s have higher biomass in 2050 (Fig. 6d). In addition, a combination of higher allocation to storage, and less to leaves, as well as lower overall understorey recruitment rates, means that those communities with high values of M_s have lower estimates of LAI (Fig. 7d). The first order impact of lower sapling mortality on biomass (more seeds = more biomass) was not present in 2005 (Fig. S3d).

The seed mixing parameter (X_m) had a large impact on community structure. Initial seeding conditions are an important control on community structure after canopy closure. When large numbers of seeds are distributed to other patches, and X_m is high, PFT1 dominance of one age class makes it a source of PFT1 seed for other age-classes, increasing its share of the seed bank and thus its increasing ability to dominate newly disturbed areas. Where most seeds land in their parent patch, and X_m is low, PFT1 wastes most of its seed increasing competition with itself. Therefore, high X_m promotes both dominance of PFT1 (Fig. 5c) and the development of communities with fast-growing PFTs. These fast-growing PFTs are at greater risk of dying under future droughted conditions because of their lower carbon reserves, so forest biomass in 2050 is lower for high X_m simulations (Fig. 6c). However, higher X_m allows faster colonization of recently disturbed gaps, facilitating faster regeneration and higher spatially averaged LAI (Fig. 7c).

Seed advection (A_s) has a relatively minor impact on community structure and on biomass in 2050 (Fig 5e, 6e). Increasing seed rain modulates the dominance of the fast-growing PFT for sapling recruitment, but also accelerates the rate of canopy closure, enhancing the dominance of the faster-growing plants (results not shown). The conflicting impact of these two mechanisms may well prevent any consistent response from emerging. A_s did have a notable impact on the biomass in 2100 (Fig. S2e), as higher seed rain presumably promotes a more rapid ecosystem recovery from mortality events (Fig. 7e). Higher seed advection also promotes higher LAI; the number of saplings present in the understorey increases on account of the shift in the equilibrium between recruitment and mortality.

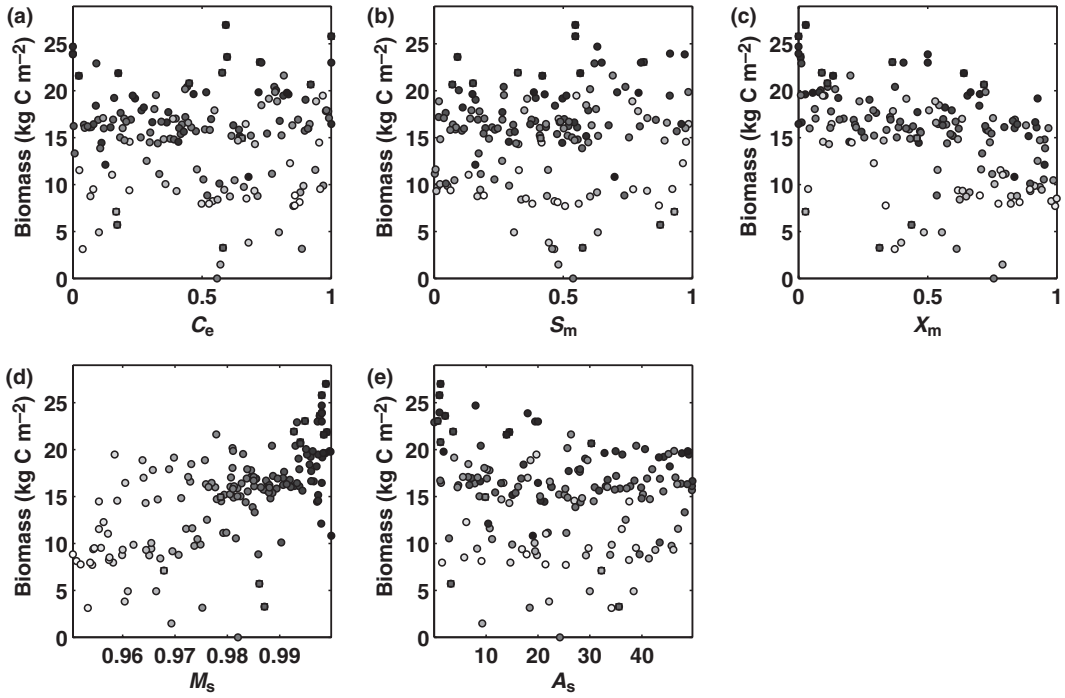

Fig. 6 Response of predicted biomass in 2050 to variation in (a) competitive exclusion, C_e, (b) stress-induced mortality, S_m, (c) seed mixing, X_m, (d) sapling mortality, M_s, and (e) seed advection, A_s. Square symbols denote members of the filtered ensemble with predictions of net primary productivity (NPP), gross primary production (GPP), leaf area index (LAI) and biomass within acceptable ranges. Shading on symbols indicates the sapling mortality parameter for each run, and can be read from panel (d).

There was little consistent effect of competitive exclusion (C_e, panel a, Figs 5 and 6) or stress-induced mortality (S_m, panel b, Figs 5 and 6) on either PFT composition (Fig 5) or biomass in 2050 (Fig 6) panel. In isolation, these parameters can exert substantial control over community structure (results not shown), but in the global sensitivity analysis (i.e. varying all parameters simultaneously) their impact may well have been overridden by large variations in the forcing caused by the other parameters. The LAI is highest for low values of S_m, as greater mortality rates of carbon-starved plants in shade or drought results in a lower equilibrium LAI (Fig. 7b).

Scale limitations and parameter constraints

Typically, vegetation modellers attempt to constrain model parameter values via observations of the processes to which they apply. Unfortunately, the parameters we investigated here are not amenable to observation because the scales at which they operate are not represented in the spatially one-dimensional model environment. For example, the rate of seed advection A_s of a given PFT is likely a function of (at least) the mean distance in space to other areas of land containing that PFT. Landscape models that include a two-dimensional spatial structure of interconnected patches, with a representation of both spatial arrangement and distance between patches, can simulate this property, but not one-dimensional DGVM models (Neilson *et al.*, 2005; Lischke *et al.*, 2006).

Similar issues apply to the other three parameters. Seed mixing, X_m, most obviously, is the result of the unknown length scale of disturbance processes and patches of land that ED represents via statistical aggregation. The length scale of ecosystem patches in reality is controlled by the size of disturbance events. If most disturbance events result from the death of single trees, this generates a matrix with a small length scale and a consequentially high rate of inter-age class seed mixing. If mortality is spatially aggregated because of blow-down events, pathogen outbreaks or fires, then the length scale will be larger and mixing less likely. No DGVM at present tracks the two-dimensional sub-grid variation in disturbance history. Tracking disturbance history is only made computationally possible in the ED model by removing the spatial dimension and tracking all patches of a common disturbance history together. This property must therefore at present be parameterized. Here we illustrate, for the first time in the context of a DGVM modelling study, how the values of this property affect model outcome. Future studies must focus on resolving this issue either using top-down observational constraints, by leveraging output from spatially explicit studies into the one-dimensional model or by converting the model framework to a substantially more computationally intensive fine-mesh structure.

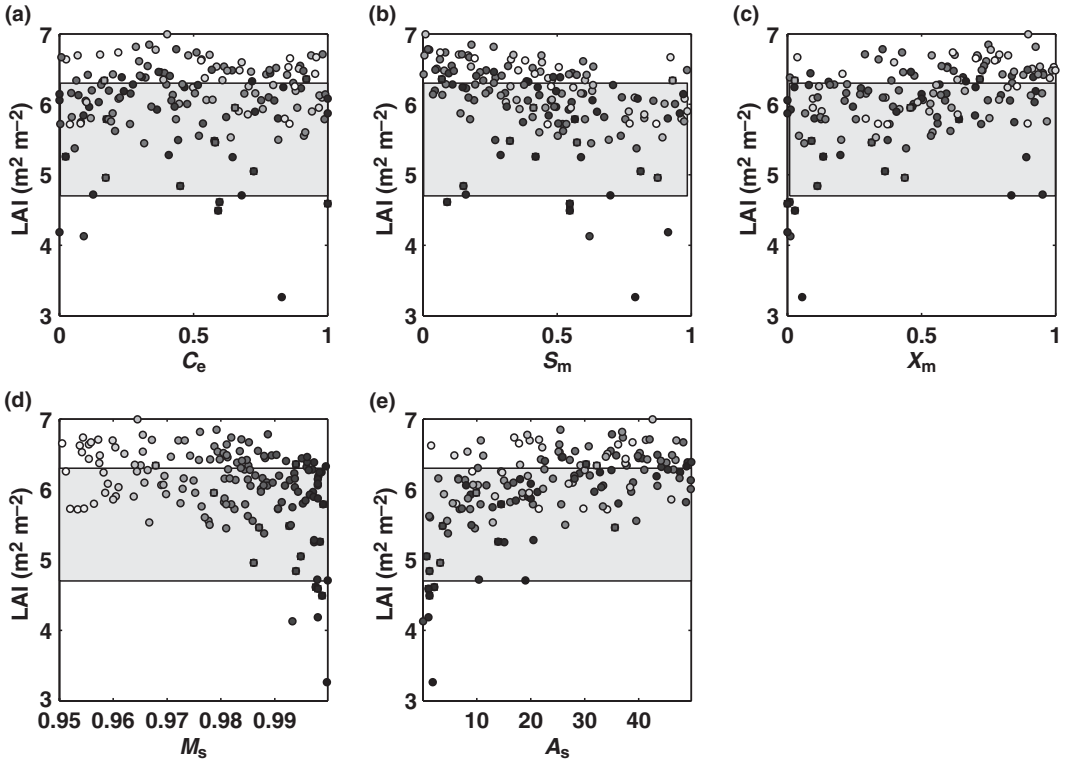

Fig. 7 Response of modelled leaf area index in 2005 to variation in (a) competitive exclusion, C_e, (b) stress-induced mortality, S_m, (c) seed mixing, X_m, (d) sapling mortality, M_s and (e) seed advection, A_s. Shaded area denotes limits of observations from Brando *et al.* (2008) and Fisher *et al.* (2007). Square symbols denote members of the filtered ensemble with predictions of net primary productivity (NPP), gross primary production (GPP), leaf area index (LAI) and biomass within acceptable ranges. Shading on symbols indicates the sapling mortality parameter for each run, and can be read from panel (d).

The degree of determinism and stochasticity of competitive exclusion, C_e, depends upon smaller-scale spatial interactions between the crowns of adjacent trees. Simulation of this process would require at least a branch-scale canopy simulation model (Williams, 1996), in addition to improved understanding of the genetic heterogeneity between plants represented by a single PFT and the microvariation in abiotic conditions. It might be possible to estimate locally appropriate values of C_e from community composition data using inverse Bayesian methods (Clark *et al.*, 2003; Etienne & Olff, 2005).

Sapling mortality, M_s, which is an aggregate of seed number, seed germination, and death of the germinated seedlings, is poorly understood and very complex to model mechanistically. Inverse estimates of seed mortality from forest inventories might be possible, but existing forest databases typically only measure trees > 10 cm diameter (Baker *et al.*, 2004). Thus, estimates of M_s are confounded with unobserved understorey growth and mortality processes. Also, sapling mortality is thought to be influenced by dispersal distance via the influence of species-specific herbivores or pathogens (Janzen, 1970; Connell, 1971) and by potential positive interactions between parent trees and saplings, the interactive consequences of which are explored by Murrell (2009).

Stress-induced mortality rates (S_m) appropriate for landscape-scale models or DGVMs are also difficult to parameterize. Allen *et al.* (2010) illustrate the difficulty of quantifying rates of vegetation mortality with observations made at multiple spatial scales. High rates of observed stand-level mortality typically translate into much lower landscape-level mortality rates, owing to spatial variation in landscape properties, biotic agents, species and weather (Allen *et al.*, 2010). For a DGVM models, that scale linearly from plot-level simulations to landscape-level prediction, the appropriate scale of measurement of plant mortality rates is therefore contentious. Landscape-level estimates of tree mortality are very rare (Allen *et al.*, 2010) but may be facilitated by vegetation monitoring networks (Phillips *et al.*, 2009) in the future.

Spatial interactions in existing studies

The concept that spatial interactions are important for community structure is not novel (Silvertown & Law, 1987) but is infrequently considered by the DGVM community (Neilson *et al.*, 2005; Midgley *et al.*, 2007). At present, no DGVMs represent the movement of propagules in two dimensions, and no first-generation DGVMs represent

plant competition for light in a vertical profile (for a detailed review of first generation DGVM plant competition algorithms see Arora & Boer, 2006). Literature from forest gap models discusses possible conditions necessary for simulating coexistence and the impact of competitive exclusion and spatial processes on community structure (Adams *et al.*, 2007; Lischke & Löffler, 2006; Kohyama & Takada, 2009) but the emerging literature on second-generation DGVMs provides little discussion on how plant coexistence is generated along axes of variation other than early-to-late successional plant traits. A vast literature on the assemblage of communities, biodiversity and species coexistence can potentially inform us on how best to proceed from this point (McGill *et al.*, 2006), and it seems likely that the possible limits on these parameters may potentially be informed by the outcomes of more spatially explicit models at various scales (Kneitel & Chase, 2004).

Conclusion

In this paper we introduce a series of modifications to the ED model that more readily allow the coexistence of plant types with similar growth rates. We conclude that, despite major advances in dynamic global vegetation modelling, there exist a number of processes pertaining to spatial plant ecology that are currently beyond the capacity of even the most sophisticated DGVMs to capture. If we fail to appropriately represent or constrain the processes that control the emergence of plant community structure in the new generation of global vegetation models, we risk generating modelled communities of plants with erroneous responses to climatic and atmospheric changes.

While we have endeavoured to create simulations that closely reflect the behaviour of Amazonian rainforest ecosystems, we emphasize that our purpose was not to provide definitive predictions of the future of the Amazon, but instead to illustrate the potential importance of the representation of infrequently discussed plant demographic processes of reproduction, competition and mortality on the range of future predictions. We chose to focus on one location to allow a detailed illustration of this high-dimension problem; however, it seems likely that the issues derived here may well be generically applicable, in different modelling frameworks, and across multiple combinations of climate and functional trade-off axes.

Acknowledgements

Funding was provided by the UK Natural Environment Research Council QUEST 'Quantifying Ecosystem's Role in the Carbon Cycle' project (QUERCC), the LANL/LDRD program and DOE Office of Science (BER) Program for Ecosystem Research. R.F. thanks Craig Allen, Doug Clark, Micheal Dietze, Manuel Gloor, Heike Lischke, Jon Lloyd, Mark Lomas, Oliver Philips, Colin Prentice, Todd Ringler, Allan Spessa, Ying-Ping Wang, Mark Westoby, Mat Williams and Ian Wright for interesting discussions that helped formulate the ideas in this manuscript.

References

Adams H, Guardiola-Claramonte M, Barron-Gafford GA, Camilo Villegas J, Breshears D, Zou CB, Troch PA, Huxman TE. 2009. Temperature sensitivity of drought-induced tree mortality portends increased regional die-off under global-change-type drought. *Proceedings of the National Academy of Sciences, USA* **106**: 7063–7066.

Adams TP, Purves DW, Pacala SW. 2007. Understanding height-structured competition in forests: is there an R^* for light? *Proceedings of the Royal Society B* **274**: 3039–3048.

Allen CD, Macalady A, Chenchouni H, Bachelet D, McDowell N, Vennetier M, Gonzales P, Hogg T, Rigling A, Breshears D *et al.* 2010. Climate-induced forest mortality: a global overview of emerging risks. *Forest Ecology and Management*. doi: 10.1016/j.foreco.2009.09.001.

Arora VK, Boer GJ. 2006. Simulating competition and coexistence between plant functional types in a dynamic vegetation model. *Earth Interactions* **10**: 1–30.

Baker TR, Philips OL, Malhi Y, Almeida S, Arroyo L, di Fiore A, Erwin T, Killeen TJ, Laurance SG, Laurance WF. 2004. Variation in wood density determines spatial patterns in Amazonian forest biomass. *Global Change Biology* **10**: 545–562.

Baraloto C, Goldberg DE, Bonal D. 2005. Performance trade-offs among tropical tree seedlings in contrasting microhabitats. *Ecology* **86**: 2461–2472.

Bonan G, Levis S, Sitch S, Vertenstein M, Oleson K. 2003. A dynamic global vegetation model for use with climate models: concepts and description of simulated vegetation dynamics. *Global Change Biology* **9**: 1543–1566.

Bonan GB. 2008. Forests and climate change: forcings, feedbacks, and the climate benefits of forests. *Science* **320**: 1444–1449.

Brando PM, Nepstad DC, Davidson EA, Trumbore SE, Ray D, Camargo P. 2008. Drought effects on litterfall, wood production and belowground carbon cycling in an Amazon forest: results of a throughfall reduction experiment. *Philosophical Transactions of the Royal Society London, Series B* **363**: 1839–1848.

Carswell FE, Costa AL, Palheta M. 2002. Seasonality in CO_2 and H_2O flux at an eastern Amazonian rain forest. *Journal of Geophysical Research* **107**: 8076.

Chao KJ, Philips OL, Gloor E, Montegud A, Torres-Lezama A, Vásquez Martínez R. 2008. Growth and wood density predict tree mortality in Amazon forests. *Journal of Ecology* **96**: 281–292.

Clark JS, Dietze M, Chakrabotry S, Agarwai PK, Ibanez I, LaDeau S, Wolosin M. 2007. Resolving the biodiversity paradox. *Ecology Letters* **10**: 647–662.

Clark JS, Mohan J, Dietze M, Ibanez I. 2003. Coexistence: how to identify trophic trade-offs. *Ecology* **84**: 17–31.

Collatz GJ, Ball JT, Grivet C, Berry JA. 1991. Physiological and environmental regulation of stomatal conductance, photosynthesis and transpiration: a model that includes a laminar boundary layer. *Agricultural and Forest Meteorology* **54**: 107–136.

Collatz GJ, Ribas-Carbo M, Berry JA. 1992. Coupled photo-synthesis stomatal conductance model for leaves of C4 plants. *Australian Journal of Plant Physiology* **19**: 519–538.

Connell JH. 1971. On the role of natural enemies in preventing competitive exclusion in some marine animals and rainforests. In: den Boer PJ, Gradwell GR, eds. *Dynamics of populations*. Wageningen, the Netherlands: PUDOC, 298–312.

Cox PM. 2001. *Description of the 'TRIFFID' dynamic global vegetation model*. Hadley Centre Technical Note no. 24, Met Office (available via http://www.metoffice.gov.uk/publications/HCTN/)

Cox PM, Betts RA, Bunton CB, Essery RLH, Rowntree PR, Smith J. 1999. The impact of new land surface physics on the GCM simulation of climate and climate sensitivity. *Climate Dynamics* **15**: 183–203.

Cox PM, Betts RA, Collins M, Harris C, Huntingford C, Jones CD. 2004. Amazon dieback under climate-carbon cycle projections for the 21st century. *Theoretical and Applied Climatology* **78**: 137–156.

Cox PM, Betts RA, Jones CD, Spall SA, Totterdell IJ. 2000. Acceleration of global warming due to carbon-cycle feedbacks in a coupled climate model. *Nature* **408**: 184–187.

Cox PM, Harris PP, Huntingford C, Betts RA, Collins M, Jones CD, Jupp TE, Marengo JA, Nobre CA. 2008. Increasing risk of Amazonian drought due to decreasing aerosol pollution. *Nature* **453**: 212–216.

Cox PM, Huntingford C, Harding RJ. 1998. A canopy conductance and photosynthesis model for use in a GCM land surface scheme. *Journal of Hydrology* **212–213**: 79–94.

Essery RLH, Best MJ, Betts RA, Cox PM, Taylor CM. 2003. Explicit representation of sub-grid heterogeneity in a GCM land-surface scheme. *Journal of Hydrometeorology* **4**: 530–543.

Etienne RS, Olff H. 2005. Confronting different models of community structure to species-abundance data: a Bayesian model comparison. *Ecology Letters*, **8**: 493–504.

Falster DS. 2006. Sapling strength and safety: the importance of wood density in tropical forests. *New Phytologist* **171**: 237–239.

Fisher RA, Williams M, Lobo do Vale R, Lola da Costa A, Meir P. 2006. Evidence from Amazonian forests is consistent with a model of isohydric control of leaf water potential. *Plant, Cell & Environment*, **29**: 151–165.

Fisher RA, Williams M, Lola da Costa A, Malhi Y, da Costa RF, Almeida S, Meir PW. 2007. The response of an Eastern Amazonian rain forest to drought stress: results and modelling analyses from a through-fall exclusion experiment. *Global Change Biology* **13**: 1–18.

Friedlingstein P, Cox P, Betts R, Bopp L *et al.* 2006. Climate-carbon cycle feedback analysis. Results form the C4MIP model inter-comparison. *Journal of Climate* **19**: 3337–3353.

Friend AD, White A. 2000. Evaluation and analysis of a dynamic terrestrial ecosystem model under preindustrial conditions at the global scale. *Global Biogeochemical Cycles* **14**: 1173–1190.

Gibon Y, Pyl ET, Sulpice R, Lunnj E, Höhne M, Günther M, Stitt M. 2009. Adjustment of growth, starch turnover, protein content and central metabolism to a decrease of the carbon supply when Arabidopsis is grown in very short photoperiods. *Plant, Cell & Environment* **32**: 859–874.

Hacke UG, Sperry JS, Wheeler JK, Castro L. 2006. Scaling of angiosperm xylem structure with safety and efficiency. *Tree Physiology* **26**: 689–701.

Harris PP, Huntingford C, Gash JHC, Hodnett MG, Cox PM, Malhi Y, Araujo AC. 2004. Calibration of a land-surface model using data from primary forest sites in Amazonia. *Theoretical and Applied Climatology* **78**: 27–45.

Hickler T, Smith B, Prentice IC, Mjöfors K, Miller P, Arneth A, Sykes MT. 2008. CO_2 fertilization in temperate forest FACE experiments not representative of boreal and tropical forests. *Global Change Biology* **14**: 1–12.

Hikosaka K. 2005. Leaf canopy as a dynamic system: ecophysiology and optimality in leaf turnover. *Annals of Botany* **95**: 521–533.

Hodnett MG, Da Silva SP, Da Rocha HR *et al.* 1995. Seasonal soil water storage changes beneath central Amazonian rainforest and pasture. *Journal of Hydrology* **170**: 233–254.

Huntingford C, Cox PM. 2000. An analogue model to derive additional climate change scenarios from existing GCM simulations. *Climate Dynamics* **16**: 575–586.

Huntingford C, Fisher RA, Mercado L, Booth BBB, Sitch S, Harris PP, Cox PM, Jones CD, Betts RA, Malhi Y *et al.* 2008. Towards quantifying uncertainty in predictions of Amazon 'dieback'. *Philosophical Transactions of the Royal Society B* **363**: 1857–1864.

Iman RL, Conover WJ. 1982. A distribution-free approach to inducing rank correlation among input variables. *Communications in Statistics* **B11**: 311–334.

Janzen DH. 1970. Herbivores and the number of tree species. *American Naturalist* **104**: 501–528.

Jipp PH, Nepstad DC, Cassel DK, De Carvalho CR. 1998. Deep soil moisture storage and transpiration in forests and pastures of seasonally-dry Amazonia. *Climatic Change* **39**: 395–412.

Jupp TE, Cox PM, Rammig A, Thonicke K, Lucht W, Cramer W. 2010. Development of probability density functions for future South American rainfall. *New Phytologist*. doi: 10.1111/j.1469-8137.2010.03368.x.

Kneitel JM, Chase JM. 2004. Trade-offs in community ecology: linking spatial scales and species coexistence. *Ecological Letters* **7**: 69–80.

Kohyama T, Takada T. 2009. The stratification theory for plant coexistence promoted by one-sided competition. *Journal of Ecology* **97**: 463–471.

Körner C. 2003. Carbon limitation in trees. *Journal of Ecology* **91**: 4–17.

Krinner G, Viovy N, de Noblet-Ducoudré N, Ogée J, Polcher J, Friedlingstein P, Ciais P, Sitch S, Prentice IC. 2005. A dynamic global vegetation model for studies of the coupled atmosphere-biosphere system. *Global Biogeochemical Cycles* **19**: GB1015, doi: 10.1029/2003GB002199.

Leibold MA, Holyoak M, Mouquet N, Amarasekare P, Chase JM, Hoopes MF, Holt RD, Shurin JB, Law R, Tilman D *et al.* 2004. The metacommunity concept: a framework for multi-scale community ecology. *Ecology Letters* **7**: 601–613.

Lischke H, Löffler TJ. 2006. Intra–specific density dependence is required to maintain species diversity in spatio-temporal forest simulations with reproduction. *Ecological Modelling* **198**: 341–361.

Lischke H, Zimmermann NE, Bolliger J, Rickebusch S, Thomas JL. 2006. TreeMig: a forest-landscape model for simulating spatio–temporal patterns from stand to landscape scale. *Ecological Modelling* **199**: 409–420.

Lloyd J, Patino S, Paiva RQ, Nardoto GB, Quesada CA, Santos AJB, Baker TR, Brand WA, Hilke I, Gielmann H *et al.* 2009. Variations in leaf physiological properties within Amazon forest canopies. *Biogeosciences Discussions* **6**: 4639–4692.

Malhi Y, Aragao LEOC, Galbraith D, Huntingford C, Fisher RA, Zelazowski P, Sitch S, McSweeney C, Meir P. 2009a. Exploring the likelihood and mechanism of a climate-change-induced dieback of the Amazon rainforest. *Proceedings of the National Academy of Sciences, USA*. doi: 10.1073/pnas.0804619106

Malhi Y, Aragão LEOC, Metcalfe DB, Paiva R, Quesada CA, Almeida S, Anderson L, Brando P, Chambers JQ, da Costa ACL *et al.* 2009b. Comprehensive assessment of carbon productivity, allocation and storage in three Amazonia forests. *Global Change Biology*. doi: 10.1111/j.1365-2486.2008.01780.x.

Malhi Y, Timmons Roberts J, Betts RA, Killeen TJ, Li W, Nobre CA. 2008. Climate change, deforestation and the fate of the Amazon. *Science* **319**: 169–172.

McDowell NG, Pockman WT, Allen CG, Breshears DD, Cobb N, Kolb T, Plaut J, Sperry J, West A, Williams DG *et al.* 2008. Mechanisms of plant survival and mortality during drought: why do some plants survive while others succumb to drought? *New Phytologist* **178**: 719–739.

McDowell NG, Sevanto S. 2010. The mechanisms of carbon starvation: how, when or does it even occur at all? *New Phytologist* **186**: 264–266.

McGill BJ, Enquist BJ, Weiher E, Westoby M. 2006. Rebuilding community ecology from functional traits. *Trends in Ecology and Evolution* **21**: 178–184.

Meir P, Cox PM, Grace J. 2006. The influence of terrestrial ecosystems on climate. *Trends in Ecology and Evolution* **21**: 254–260.

Meir P, Metcalfe DB, Costa ACL. 2008. The fate of assimilated carbon during drought: impacts on respiration in Amazon rain forests. *Philosophical Transactions of the Royal Society London, Series B* **363**: 1849–1855.

Metcalfe DB, Meir P, Aragão LEOC, Lobo-do-Vale R, Galbraith D, Fisher RA, Chaves MM, Maroco JP, da Costa ACL, de Almeida SS *et al.* 2010. Shifts in plant respiration and carbon use efficiency at a large-scale drought experiment in the eastern Amazon. *New Phytologist*. doi: 10.1111/j.1469-8137.2010.03319.x

Mercado LM, Bellouin N, Sitch S, Boucher O, Huntingford C, Wild M, Cox PM. 2009. Impact of changes in diffuse radiation on the global land carbon sink. *Nature* **458**: 1014–1018.

Mercado LM, Huntingford C, Gash JHC, Cox PM, Jogireddy V. 2007. Improving the representation of radiation interception and photosynthesis for climate model applications. *Tellus B* **59**: 553–565.

Midgley GF, Thuiller W, Higgins SI. 2007. Plant species migration as a key uncertainty in predicting future impacts of climate change on ecosystems: progress and challenges in terrestrial ecosystems in a changing world, global change – The IGBP series. In: Canadell JG, Pataki DE, Pitelka LF, eds. *Terrestrial Ecosystems in a Changing World*. Berlin Heidelberg, Germany: Springer 128–137.

Moorcroft PR. 2006. How close are we to a predictive science of the biosphere? *Trends in Ecology and Evolution* **21**: 400–407.

Moorcroft PR, Hurtt GC, Pacala SW. 2001. A method for scaling vegetation dynamics: the ecosystem demography model (ED). *Ecological Monographs* **71**: 557–586.

Murrell DJ. 2009. On the emergent spatial structure of size-structured populations: when does self-thinning lead to a reduction in clustering? *Journal of Ecology* **97**: 256–266.

Neilson RP, Pitelka LF, Solomon AM, Nathan R, Midgley GF, Fragoso JMV, Lischke H, Thompson K. 2005. Forecasting regional to global plant migration in response to climate change. *Bioscience* **55**: 749–759.

Nepstad DC, Decarvalho CR, Davidson EA, Jipp PH, Lefebvre PA, Negreiros GH, Dasilva ED, Stone TA, Trumbore SE, Vieira S. 1994. The role of deep roots in the hydrological and carbon cycles of Amazonian forests and pastures. *Nature* **372**: 666–669.

Nepstad DC, Sitckler CM, Soares-Filho B, Merry F. 2008. Interactions among Amazon land use, forests and climate: prospects for a near-term forest tipping point. *Philosophical Transactions of the Royal Society. Series B* **363**: 1737–1746.

Osada N, Takeda H, Kitajima K, Pearcy R. 2003. Functional correlates of leaf demographic response to gap release in saplings of a shade-tolerant tree *Elateriospermum tapos*. *Oecologia* **137**: 181–187.

Pacala SW, Canham CD, Saponara J, Silander JA Jr, Kobe RK, Ribbens E. 1996. Forest models defined by field measurements: estimation, error analysis, and dynamics. *Ecological Monographs* **66**: 1–44.

Phillips OL, Aragão LEOC, Lewis SL, Fisher JB, Lloyd J, López-González G, Malhi Y, Monteagudo A, Peacock J, Quesada CA, *et al.* 2009. Drought sensitivity of the Amazon rainforest. *Science* **323**: 1344–1347.

Poorter L, McDonald I, Alarcón A, Fichtler E, Licona JC, Peña-Claros M, Sterck F, Villegas Z, Sass-Klaassen U. 2010. The importance of wood traits and hydraulic conductance for the performance and life history strategies of 42 rainforest tree species. *New Phytologist* **185**: 481–492.

Prentice IC, Bondeau A, Cramer W, Harrison SP, Hickler T, Lucht W, Sitch S, Smith B, Sykes MT. 2007. Dynamic global vegetation modeling: quantifying terrestrial ecosystem responses to large-scale environmental change. In: Canadell JG, Pataki DE, Pitelka LF, eds. *Terrestrial ecosystems in a changing world*. Berlin Heidelberg, Germany: Springer, doi: 10.1007/978-3-540-32730-1_15

Purves DW, Lichstein JW, Pacala SW. 2008a. Crown plasticity and competition for canopy space: a new spatially implicit model parameterized for 250 North American tree species. *PLoS-One* **2**: e870.

Purves DW, Lichstein JW, Strigul N, Pacala SW. 2008b. Predicting and understanding forest dynamics using a simple tractable model. *Proceedings of the National Academy of Sciences, USA* **105**: 17018–17022.

Purves DW, Pacala S. 2008. Predictive models of forest dynamics. *Science* **320**: 1452–1453.

Randerson JT, Hoffman FM, Thornton PE, Mahowald NM, Lindsay K, Lee YH, Nevison CD, Doney SC, Bonan G, Stöckli R *et al.* 2009. Systematic assessment of terrestrial biogeochemistry in coupled climate–carbon models. *Global Change Biology* **15**: 2462–2484.

Reich PB, Wright IJ, Lusk CH. 2007. Predicting leaf physiology from simple plant and climate attributes: a global GLOPNET analysis. *Ecological Applications* **17**: 1982–1988.

da Rocha HR, Goulden ML, Miller SD, Menton MC, Pinto Ldvo, de Freitas HC, Figueira A. 2004. Seasonality of water and heat fluxes over a tropical forest in eastern Amazonia. *Ecological Applications* **14**: S22–S32.

Rodenbeck C, Houweling S, Gloor M, Heimann M. 2003. CO_2 flux history 1982–2001 inferred from atmospheric data using a global inversion of atmospheric transport. *Atmospheric Chemistry and Physics* **3**: 1919–1964.

Sala A, Piper F, Hoch G. 2010. Physiological mechanisms of drought-induced tree mortality are far from being resolved. *New Phytologist* **186**: 274–281.

Salazar LF, Nobre CA, Oyama MD. 2007. Climate change consequences on the biome distribution in tropical South America. *Geophysical Research Letters* **34**. URL http://www.agu.org/pubs/crossref/2007.../2007GL029695.shtml [accessed on 23 June 2010].

Sato H, Itoh A, Kohyama T. 2007. SEIB–DGVM: a new dynamic global vegetation model using a spatially explicit individual-based approach. *Ecological Modeling* **200**: 279–307.

Scheiter S, Higgins SI. 2008. Impacts of climate change on the vegetation of Africa: an adaptive dynamic vegetation modelling approach. *Global Change Biology* **15**: 2224–2246.

Selaya NG, Oomen RJ, Netten JJC, Werger MJA, Anten NPR. 2008. Biomass allocation and leaf life span in relation to light interception by tropical forest plants during the first years of secondary succession. *Journal of Ecology* **96**: 1211–1221.

Sellers PJ, Berry JA, Collatz GJ, Field CB, Hall FG. 1992. Canopy reflectance, photosynthesis and transpiration III: a reanalysis using improved leaf models and a new canopy integration scheme. *Remote Sensing and Environment* **42**: 187–216.

Sellers PJ, Mintz Y, Sub YC, Dalcher A. 1986. A simple biosphere model (SiB) for use within general circulation models. *Journal of Atmospheric Science* **43**: 505–531.

Silvertown J, Law R. 1987. Do plants need niches? Some recent developments in plant community ecology. *Trends in Ecology and Evolution* **2**: 24–26.

Sitch S, Huntingford C, Gedney N, Levy PE, Lomas M, Piao SL, Betts R, Ciais P, Cox P, Friedlingstein P *et al.* 2008. Evaluation of the terrestrial carbon cycle, future plant geography and climate-carbon cycle feedbacks using five dynamic global vegetation models (DGVMs). *Global Change Biology* **14**: 1–25.

Sitch S, Smith B, Prentice IC, Arneth A, Bondeau A, Cramer W, Kaplans JW, Levis S, Lucht W, Sykes MT, *et al.* 2003. Evaluation of ecosystem

dynamics, plant geography and terrestrial carbon cycling in the LPJ dynamic vegetation model. *Global Change Biology* **9**: 161–185.

Smith AM, Stitt M. 2007. Coordination of carbon supply and plant growth. *Plant, Cell & Environment* **30**: 1126–1149.

Smith B, Prentice IC, Sykes MT. 2001. Representation of vegetation dynamics in modelling of terrestrial ecosystems: comparing two contrasting approaches within European climate space. *Global Ecology and Biogeography* **10**: 621–637.

Sperry JS, Adler FR, Campbell GS, Comstock JP. 1998. Limitation of plant water use by rhizosphere and xylem conductance: results from a model. *Plant, Cell & Environment* **21**: 47–359.

Thornton PE, Lamarque J-F, Rosenbloom NA, Mahowald NM. 2007. Influence of carbon–nitrogen cycle coupling on land model response to CO_2 fertilization and climate variability. *Global Biogeochemical Cycles*, **21**, GB4018, doi: 10.1029/2006GB002868

Williams M. 1996. A three-dimensional model of forest development and competition. *Ecological Modelling* **89**: 73–98.

Woodward FI, Lomas MR. 2004. Vegetation-dynamics – simulating responses to climate change. *Biological Reviews* **79**: 643–670.

Wright IJ, Reich PB, Westoby M, Ackerly DD, Baruch Z, Bongers F, Cavender-Bares J, Chapin T, Cornelissen JHC, Diemer M *et al.* 2004. The world-wide leaf economics spectrum. *Nature* **428**: 821–827.

Würth MKR, Pelaez-Riedl S, Wright SJ, Korner C. 2005. Non-structural carbohydrate pools in a tropical forest. *Oecologia* **143**: 11–24.

Zeng N, Mariotti A, Wetzel P. 2005. Terrestrial mechanisms of interannual CO_2 variability. *Global Biogeochemical Cycles* **19**: GB1016. (doi: 101029/2004GB002273).

Supporting Information

Additional supporting information may be found in the online version of this article.

Fig. S1 Response of predicted biomass at year 2005 to variation in (a) competitive exclusion, C_e, (b) stress-induced mortality, S_m, (c) seed mixing, X_m, (d) sapling mortality, M_s, and (e) seed advection, A_s.

Fig. S2 Response of predicted biomass at year 2100 to variation in (a) competitive exclusion, C_e, (b) stress-induced mortality, S_m, (c) seed mixing, X_m, (d) sapling mortality, M_s, and (e) seed advection, A_s.

Fig. S3 Response of predicted gross primary production (GPP) at year 2100 to variation in (a) competitive exclusion C_e, (b) stress-induced mortality, S_m, (c) seed mixing, X_m, (d) sapling mortality, M_s, and (e) seed advection, A_s.

Fig. S4 Response of predicted net primary productivity (NPP) at year 2100 to variation in (a) competitive exclusion, C_e, (b) stress-induced mortality, S_m, (c) seed mixing, X_m, (d) sapling mortality, M_s, and (e) seed advection, A_s.

Notes S1 Detailed description of JULES gas exchange model and algorithms controlling tree leaf area, canopy spread and physiological gradients within the forest canopy.

Please note: Wiley-Blackwell are not responsible for the content or functionality of any supporting information supplied by the authors. Any queries (other than missing material) should be directed to the *New Phytologist* Central Office.